Available online at www.sciencedirect.com
SCIENCE DIRECT
Journal of Sound and Vibration 296 (2006) 209–225
JOURNAL OF SOUND AND VIBRATION
www.elsevier.com/locate/jsvi

# The frequency dependence of jet turbulence for noise source modelling

F. Kerhervé[a], J. Fitzpatrick[a,*], P. Jordan[b]

[a]*Mechanical and Manufacturing Engineering Department, Trinity College, Ireland*
[b]*Laboratoire d'Etudes Aérodynamiques UMR CNRS 6609, Poitiers, France*

Received 19 April 2005; received in revised form 20 February 2006; accepted 22 February 2006
Available online 8 May 2006

**Abstract**

The turbulence statistics of high speed jets provide a basis for modelling the source mechanisms responsible for noise generation. Progress in recent years where a statistical approach has been used includes better modelling of the subtler aspects of the turbulence field constituted by high speed jets, including anisotropy, inhomogeneity and the frequency dependence of the integral scales. In this paper, the frequency dependence of the length and time scales and the convection velocity are considered in order to provide improved turbulence models for the prediction of sound. It is shown that the use of a complex coherence function enables the frequency dependence of the turbulence scales to be established analytically. The frequency-dependent length scale is shown to be determined from the real part of this coherence function while the frequency-dependent time scale in the moving frame of reference is obtained from the modulus with the convection speed given by the phase. The results for the frequency dependence of the turbulence properties derived from two-point laser Doppler velocimetry measurements in high speed subsonic jets are presented and shown to agree well with those from an analytical model based on a Gaussian form for the two point correlation. The implications of the results in respect of noise prediction methodologies are discussed.


## 1. Introduction

The use of the Lighthill acoustic analogy [1] for jet noise prediction remains the preferred technique in the aerospace industrial community. This imposes a number of restrictive assumptions which can render predictions inaccurate, particularly where complex flows constituted by modern high-by-pass engines with enhanced mixing devices are concerned. Acoustic analogy methods for jet noise are based on the spatio-temporal correlation tensor of the turbulence. This is a complex four-dimensional function in the case of jet noise, for which a general analytical form is only available if the turbulence is considered either homogeneous and isotropic or axisymmetric. The accuracy of a noise prediction will depend critically on the accuracy with which this quantity can be modelled as the error incurred by simplified models may be greater than the

*Corresponding author. Tel.: +353 1 608 1778; fax: +353 8 679 5554.
*E-mail addresses:* kerherf@tcd.ie (F. Kerhervé), john.fitzpatrick@tcd.ie (J. Fitzpatrick), peter.jordan@lea.univ-poitiers.fr (P. Jordan).

0022-460X/$ - see front matter 
doi:10.1016/j.jsv.2006.02.012

**Nomenclature**

| | |
|---|---|
| $c_0$ | sound speed in medium at rest |
| $\mathbf{k}_w$ | wavenumber vector |
| $L_c$ | potential core length |
| $r^*_{ij}$ | second-order spatio-temporal correlation tensor |
| $r_{ij}$ | normalised second-order spatio-temporal correlation tensor |
| $r^*_{ijkl}$ | fourth-order spatio-temporal correlation tensor |
| $r_{ijkl}$ | normalised fourth-order spatio-temporal correlation tensor |
| $\mathbf{s}$ | separation vector |
| $\mathbf{s}_k$, $s_k$ | $k$th component of $\mathbf{s}$ and its modulus |
| $S_i(\mathbf{y},\omega)$ | auto-power spectrum of $u_i$ |
| $S_{ij}(\mathbf{y},\mathbf{s},\omega)$ | cross-power spectral tensor of $u_i$ and $u_j$ |
| $St$ | Strouhal number |
| $t$ | time |
| $u_i$ | $i$th component of the fluctuating velocity field |
| $\mathbf{u}^k_c$ | $k$th component of the frequency-dependent convection velocity |
| $U_c$ | convection velocity in the mainstream direction |
| $\mathbf{U}^k_c, U^k_c$ | $k$th component of the convection velocity and its modulus |
| $\mathbf{x}$ | position of the observer in the far field |
| $x_i$ | magnitude of the $i$th component of $\mathbf{x}$ |
| $W(x,\omega)$ | acoustic power radiated in the far field |
| $\mathbf{y}$ | source coordinate into the flow |
| $\gamma_{ij}$ | complex coherence function |
| $\nabla_\omega$ | double-sided bandpass filter |
| $\Lambda^k_{ij}, \tau^k_{ij}$ | space and time integral scales in the $k$th direction |
| $\Lambda^k_{ij}[\mathbf{y},\omega], \tau^k_{ij}[\mathbf{y},\omega]$ | $k$th component of the frequency-dependent turbulence scales |
| $\rho, \rho_0$ | local density and value in the medium at rest |
| $\tau$ | time delay |
| $\omega$ | radian frequency |

acoustic energy to be predicted. Thus to optimise this kind of approach it is important to incorporate as much of the flow physics as possible into the model.

One aspect of the flow dynamic which is not addressed by time-domain representations of this correlation tensor is the multi-scale character of the turbulence. As suggested by Townsend [2], the turbulence field can be seen as a "superposition of many eddies of different kinds, sizes and orientations", which will be characterised by a range of different length and time scales. Harper-Bourne [3], Morris and Boluriaan [4] and Self [5] have recently sought to include this frequency dependence in statistical noise prediction methodologies, and have shown how improvement in prediction accuracy is possible if this multi-scale character is accounted for, via formulation of Lighthill's acoustic analogy in the frequency domain. The superiority of this kind of approach lies not solely in terms of an enhanced prediction capacity, but also in terms of the improved physical insight which can be provided as to the importance of the various turbulence quantities involved in the production and radiation of jet noise. For turbulent boundary layers, Durant et al. [6] used the coherence function between two pressure measurements together with the phase of their cross-spectrum to establish a model for induced pressure fluctuations.

In this work, the frequency dependence of the space scales and the convection velocities is derived analytically and related to the integral scales of the turbulence. This approach differs from that of Harper-Bourne [3] and Morris and Boluriaan [4] as, in their work, the frequency dependence was not explicitly related to these flow quantities. Furthermore, it is demonstrated how in their formulation the frequency dependence derived corresponds not in fact to the turbulence length scale, but rather to a projection of the moving-frame *time-scale* onto the spatial dimension. The correct model is derived, discussed and compared with measurements performed using two-point Laser Doppler Velocimetry (LDV) in the mixing region of hot and isothermal high speed jets.

## 2. Theoretical background

Using the Lighthill acoustic analogy, the sound pressure intensity radiated by free turbulence can be written as

$$W(x,\omega) = \frac{x_i x_j x_k x_l}{16\pi^2 \rho_0 c_0^5 |\mathbf{x}|^6} \omega^4 \int_{V_y} \int_{V_s} S_{ijkl}(\mathbf{y},\mathbf{s},\omega) \mathrm{e}^{-j\mathbf{k}_w\cdot\mathbf{s}} \,\mathrm{d}^3\mathbf{y}\,\mathrm{d}^3\mathbf{s}, \tag{1}$$

where the sound field is represented in the frequency domain and the source field in wavenumber–frequency space. $S_{ijkl}$ is a cross-spectral tensor for the Reynolds stresses $u_iu_j$ and $u_ku_l$ at locations separated by the vector $\mathbf{s}$. The vector $\mathbf{y}$ denotes a source region coordinate at which this tensor is evaluated, $\mathbf{k}_w$ is the wavenumber vector given by $\omega\mathbf{y}/|\mathbf{y}|c_0$, $\rho_0$ and $c_0$ are, respectively, the density and sound speed in the medium at rest.

The time domain equivalent of this spectral tensor is the fourth-order spatio-temporal velocity correlation given by

$$R_{ijkl}(\mathbf{y},\mathbf{s},\tau)=\overline{\rho^2}\,\overline{u_iu_j(\mathbf{y},t)u_ku_l(\mathbf{y}+\mathbf{s},t+\tau)}, \tag{2}$$

where the overbar denotes a time average and $u_i$ is the $i$th component of the instantaneous turbulence velocity.

An exact estimation of the Reynolds stress tensor requires the variation of the density to be know locally. For the present work, incompressible jets are investigated so the dynamic of the turbulence field can be defined by the fluctuating velocities only and local variations of density are not considered so that the fourth-order correlation tensor reduces to

$$r^*_{ijkl}(\mathbf{y},\mathbf{s},\tau)=\overline{u_iu_j(\mathbf{y},t)u_ku_l(\mathbf{y}+\mathbf{s},t+\tau)}. \tag{3}$$

Although Lighthill [7] suggested that a statistical assumption was unnecessary, this is in fact not the case and an assumption of normal joint probability needs to be made for the turbulence statistics at locations $\mathbf{y}$ and $\mathbf{y}+\mathbf{s}$ so that the fourth-order velocity correlation tensor can be expressed as the sum of second-order tensor products as

$$r^*_{ijkl}(\mathbf{y},\mathbf{s},\tau)=r^*_{ik}(\mathbf{y},\mathbf{s},\tau)r^*_{jl}(\mathbf{y},\mathbf{s},\tau)+r^*_{il}(\mathbf{y},\mathbf{s},\tau)r^*_{jk}(\mathbf{y},\mathbf{s},\tau). \tag{4}$$

Freund [8] has shown that this approximation is appropriate in a low Reynolds number jet and argued that it should also hold at higher Reynolds numbers. The Fourier transform of this gives the corresponding cross-spectral tensors $S_{ij}(\mathbf{y},\mathbf{s},\omega)$ which will then appear in the frequency domain representation of the Lighthill formulation given by Eq. (1). Modelling the source term thus requires modelling of either $r_{ij}(\mathbf{y},\mathbf{s},\tau)$ or $S_{ij}(\mathbf{y},\mathbf{s},\omega)$, which are representative of the source dynamic, and will influence the accuracy of a noise prediction model. As the sound production mechanism for jet noise is considered to comprise contributions from both the large-scale dynamic of the flow (important for the peak radiation directions) and from the dynamic of the smaller scales (considered important for sideline noise), then explicit inclusion of the different scales is important if the true flow physics responsible for the noise generation mechanisms are to be correctly estimated.

## 3. Frequency dependence of the source mechanism

The space and time scales of a turbulence field, noted $\Lambda^k_{ij}$ and $\tau^k_{ij}$, respectively, are commonly derived from the normalised two-point correlation $r_{ij}$ as

$$\Lambda^k_{ij}=\int_0^{+\infty} r_{ij}(\mathbf{y},\mathbf{s}_k,\tau=0)\,\mathrm{d}s_k, \tag{5}$$

$$\tau^k_{ij}=\int_0^{+\infty} r_{ij}(\mathbf{y},\mathbf{s}_k=\mathbf{U}^k_c\tau,\tau)\,\mathrm{d}\tau, \tag{6}$$

where

$$r_{ij}(\mathbf{y},\mathbf{s},\tau)=\frac{r^*_{ij}(\mathbf{y},\mathbf{s},\tau)}{[\overline{u_i(\mathbf{y},t)^2}\cdot\overline{u_j(\mathbf{y}+\mathbf{s},t+\tau)^2}]^{1/2}}, \tag{7}$$

with

$$r^*_{ij}(\mathbf{y},\mathbf{s},\tau)=\overline{u_i(\mathbf{y},t)u_j(\mathbf{y}+\mathbf{s},t+\tau)}, \tag{8}$$

where $k$ denotes the direction of the separation vector, $i$ and $j$ are the components of the turbulence velocity and the inclusion of the convection velocity, $U_c$, ensures that it is the turbulence in the moving frame of reference which is considered. The overbar denotes a time average.

The frequency dependence of these scales is of interest and so the space–time correlation function $r^*_{ij}$ must be considered in the frequency domain, where it becomes the cross-power spectral density function, $S_{ij}(\mathbf{y}, \mathbf{s}_k, \omega)$. This relationship is given by

$$r^*_{ij}(\mathbf{y}, \mathbf{s}_k, \tau) = \frac{1}{2\pi} \int_{-\infty}^{+\infty} S_{ij}(\mathbf{y}, \mathbf{s}_k, \omega) \mathrm{e}^{\mathrm{j}\omega\tau} \, \mathrm{d}\omega. \tag{9}$$

The variances of the velocity field at both locations can be expressed in terms of the auto-power spectral densities as

$$\overline{u_i(\mathbf{y}, t)^2} = \frac{1}{2\pi} \int_{-\infty}^{+\infty} S_i(\mathbf{y}, \omega) \, \mathrm{d}\omega,$$

$$\overline{u_j(\mathbf{y} + \mathbf{s}_k, t)^2} = \frac{1}{2\pi} \int_{-\infty}^{+\infty} S_j(\mathbf{y} + \mathbf{s}_k, \omega) \, \mathrm{d}\omega \tag{10}$$

and so, the integrands in Eqs. (5) and (6) can be expressed as

$$r_{ij}(\mathbf{y}, \mathbf{s}, \tau = 0) = \int_{-\infty}^{+\infty} S_{ij}(\mathbf{y}, \mathbf{s}, \omega) \, \mathrm{d}\omega \left[ \int_{-\infty}^{+\infty} S_i(\mathbf{y}, \omega) \, \mathrm{d}\omega \int_{-\infty}^{+\infty} S_j(\mathbf{y} + \mathbf{s}, \omega) \, \mathrm{d}\omega \right]^{-1/2}, \tag{11}$$

$$r_{ij}(\mathbf{y}, \mathbf{s} = \mathbf{U}_c\tau, \tau) = \int_{-\infty}^{+\infty} S_{ij}(\mathbf{y}, \mathbf{U}_c\tau, \omega) \mathrm{e}^{\mathrm{j}\omega\tau} \, \mathrm{d}\omega \left[ \int_{-\infty}^{+\infty} S_i(\mathbf{y}, \omega) \, \mathrm{d}\omega \int_{-\infty}^{+\infty} S_j(\mathbf{y} + \mathbf{U}_c\tau, \omega) \, \mathrm{d}\omega \right]^{-1/2}. \tag{12}$$

A typical representation of these integrands is reported in Fig. 1. Formulated in this way the frequency dependence of the source term which appears explicitly in Eq. (1) can be examined. In terms of the noise source mechanisms, the spatial part (Eq. (11)), is subject to a volumetric integral in Eq. (1) and relates to the spatial extent over which the turbulence is correlated. On the other hand, the temporal part (Eq. (12)), subject to a double differentiation in Eq. (1), gives the importance of the dynamic of the turbulence in the convective reference-frame. When viewed in spectral terms these can be considered in terms of the individual Fourier components. For aeroacoustic sources, the spatial part is a measure of the typical volumetric extent over which different turbulence scales are efficient in the conversion of hydrodynamic kinetic energy into acoustic energy and the temporal part gives the dynamic of that conversion. As an aside it is worth mentioning that in

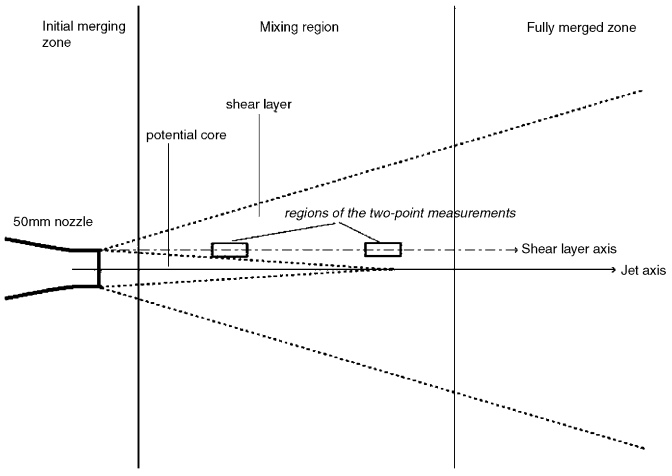


Fig. 1. Jet schematic.

addition to providing a means of effecting a low-cost estimation of the sound produced by turbulence, this kind of statistical approach can give good physical insight into the mechanisms responsible for the generation of sound.

### 3.1. Frequency dependence of the length scale

Substitution of Eq. (11) into Eq. (5) leads to an expression for the integral length scale in which the frequency appears explicitly

$$\Lambda_{ij}^{k} = \int_{0}^{+\infty} \int_{-\infty}^{+\infty} S_{ij}(\mathbf{y}, \mathbf{s}_k, \omega)\, \mathrm{d}\omega \left[ \int_{-\infty}^{+\infty} S_i(\mathbf{y}, \omega)\, \mathrm{d}\omega \int_{-\infty}^{+\infty} S_j(\mathbf{y}+\mathbf{s}_k, \omega)\, \mathrm{d}\omega \right]^{-1/2} \mathrm{d}\mathbf{s}_k. \tag{13}$$

In order to determine the frequency dependence of the length scales, an operation analogous to the bandpass filtering of experimental data, as used for example by Fisher and Davies [9] or as discussed by Lumley and Takeuchi [10] can be implemented. Using a double-sided bandpass filter $\nabla_{\omega'}$ defined by

$$\nabla_{\omega'}(\omega) = \begin{cases} 1 & \text{for } \omega \in [-\omega' - \delta\omega, -\omega' + \delta\omega] \text{ or } [\omega' - \delta\omega, \omega' + \delta\omega], \\ 0 & \text{otherwise,} \end{cases}$$

leads to length scales which can be associated with the spectral components of the turbulence centred at $\omega'$ and spanning $2\delta\omega$. This can be written as

$$\begin{aligned} \Lambda_{ij}^{k}[\omega, \nabla_{\omega'}] = \int_{0}^{+\infty} \Bigg[ & \int_{-\infty}^{+\infty} \nabla_{\omega'}(\omega) S_{ij}(\mathbf{y}, \mathbf{s}_k, \omega)\, \mathrm{d}\omega \\ & \times \left[ \int_{-\infty}^{+\infty} \nabla_{\omega'}(\omega) S_i(\mathbf{y}, \omega)\, \mathrm{d}\omega \int_{-\infty}^{+\infty} \nabla_{\omega'}(\omega) S_j(\mathbf{y}+\mathbf{s}_k, \omega)\, \mathrm{d}\omega \right]^{-1/2} \Bigg] \mathrm{d}\mathbf{s}_k. \end{aligned} \tag{14}$$

The terms on the right-hand side of this equation can be written as

$$\begin{aligned} \int_{-\infty}^{+\infty} \nabla_{\omega'}(\omega) S_{ij}(\mathbf{y}, \mathbf{s}_k, \omega)\, \mathrm{d}\omega &= \int_{-\omega'-\delta\omega}^{-\omega+\delta\omega} S_{ij}(\mathbf{y}, \mathbf{s}_k, \omega)\, \mathrm{d}\omega + \int_{\omega'-\delta\omega}^{\omega+\delta\omega} S_{ij}(\mathbf{y}, \mathbf{s}_k, \omega)\, \mathrm{d}\omega, \\ \int_{-\infty}^{+\infty} \nabla_{\omega'}(\omega) S_i(\mathbf{y}, \omega)\, \mathrm{d}\omega &= \int_{-\omega'-\delta\omega}^{-\omega'+\delta\omega} S_i(\mathbf{y}, \omega)\, \mathrm{d}\omega + \int_{\omega'-\delta\omega}^{\omega'+\delta\omega} S_i(\mathbf{y}, \omega)\, \mathrm{d}\omega, \end{aligned} \tag{15}$$

so that, in the limit the frequency-dependent length scale is given by

$$\Lambda_{ij}^{k}(\mathbf{y}, \omega') = \int_{0}^{+\infty} \frac{S_{ij}(\mathbf{y}, \mathbf{s}_k, -\omega') + S_{ij}(\mathbf{y}, \mathbf{s}_k, \omega')}{[(S_i(\mathbf{y}, -\omega') + S_i(\mathbf{y}, \omega'))(S_j(\mathbf{y}+\mathbf{s}_k, -\omega') + S_j(\mathbf{y}+\mathbf{s}_k, \omega'))]^{1/2}}\, \mathrm{d}\mathbf{s}_k. \tag{16}$$

As the auto-power spectral density function is an even function of the frequency this leads to

$$S_i(\mathbf{y}, -\omega') + S_i(\mathbf{y}, \omega') = 2S_i(\mathbf{y}, \omega'). \tag{17}$$

Also, since the imaginary part of the cross-power spectral density is an odd function of the frequency, this gives,

$$S_{ij}(\mathbf{y}, \mathbf{s}_k, -\omega') + S_{ij}(\mathbf{y}, \mathbf{s}_k, \omega') = 2\mathrm{Re}[S_{ij}(\mathbf{y}, \mathbf{s}_k, \omega')]. \tag{18}$$

A complex coherence function between the turbulence velocity components $i$ and $j$ at locations $\mathbf{y}$ and $\mathbf{y}+\mathbf{s}_k$ for the Fourier component $\omega'$ can now be defined as

$$\gamma_{ij}(\mathbf{y}, \mathbf{s}_k, \omega') = \frac{S_{ij}(\mathbf{y}, \mathbf{s}_k, \omega')}{[S_i(\mathbf{y}, \omega') S_j(\mathbf{y}+\mathbf{s}_k, \omega')]^{1/2}}. \tag{19}$$

From this last equation, it can be seen that the frequency dependence of the length scale as given in Eq. (16) depends on the real part of this function and is given by

$$\Lambda_{ij}^{k}(\mathbf{y},\omega') = \int_0^{+\infty} \mathrm{Re}[\gamma_{ij}(\mathbf{y},\mathbf{s}_k,\omega')]\,\mathrm{d}s_k \tag{20}$$

Although Wills [11] made a statement to this effect, he did not provide an analytical demonstration. It should further be noted that this result is not the same as using the magnitude of the coherence to obtain the frequency dependence of the length scales. It can be shown how use of the coherence magnitude gives an estimation of the frequency dependence of a quantity which is related to the moving-frame time scale rather than the spatial scales of the turbulence. This can be demonstrated by examining the frequency dependence of the time scale.

### 3.2. Frequency dependence of the moving-frame time scale

The frequency domain representation of the integral time scale can be obtained from Eq. (12) as

$$\tau_{ij}^{k} = \int_0^{+\infty}\int_{-\infty}^{+\infty} S_{ij}(\mathbf{y},\mathbf{U}_c^k\tau,\omega)\mathrm{e}^{\mathrm{j}\omega\tau}\,\mathrm{d}\omega \times\left[\int_{-\infty}^{+\infty} S_i(\mathbf{y},\omega)\,\mathrm{d}\omega\int_{-\infty}^{+\infty} S_j(\mathbf{y}+\mathbf{U}_c^k\tau,\omega)\,\mathrm{d}\omega\right]^{-1/2}\mathrm{d}\tau. \tag{21}$$

Expressing the cross-spectrum $S_{ij}$ in terms of magnitude and phase, this can be written as

$$\tau_{ij}^{k} = \int_0^{+\infty}\int_{-\infty}^{+\infty} |S_{ij}(\mathbf{y},\mathbf{U}_c^k\tau,\omega)|\mathrm{e}^{-j\Phi_k}\mathrm{e}^{\mathrm{j}\omega\tau}\,\mathrm{d}\omega \times\left[\int_{-\infty}^{+\infty} S_i(\mathbf{y},\omega)\,\mathrm{d}\omega\int_{-\infty}^{+\infty} S_j(\mathbf{y}+\mathbf{U}_c^k\tau,\omega)\,\mathrm{d}\omega\right]^{-1/2}\mathrm{d}\tau \tag{22}$$

where $\Phi_k$ is the phase of the cross-spectrum between two points in the $k$th-direction, given by $\Phi_k = \omega s_k/U_c^k$. Since in the convected reference-frame the space and time coordinates are related by the convection velocity (i.e. $s_k/U_c^k = \tau$), the exponentials in the first integrand vanish such that this equation becomes

$$\tau_{ij}^{k} = \int_0^{+\infty}\int_{-\infty}^{+\infty} |S_{ij}(\mathbf{y},\mathbf{U}_c^k\tau,\omega)|\,\mathrm{d}\omega \times\left[\int_{-\infty}^{+\infty} S_i(\mathbf{y},\omega)\,\mathrm{d}\omega\int_{-\infty}^{+\infty} S_j(\mathbf{y}+\mathbf{U}_c^k\tau,\omega)\,\mathrm{d}\omega\right]^{-1/2}\mathrm{d}\tau. \tag{23}$$

Using the same procedure as for the frequency dependence of the length scale between Eqs. (13) and (18), the frequency dependence of the time-scale can now be obtained as the modulus of the complex coherence function given by

$$\tau_{ij}^{k}(\mathbf{y},\omega') = \int_0^{+\infty} |\gamma_{ij}(\mathbf{y},\mathbf{u}_c^k(\boldsymbol{\omega})\tau,\omega')|\,\mathrm{d}\tau. \tag{24}$$

It should be noted that the global convection velocity is replaced by a frequency-dependent convection velocity, translating the fact that the various scales are convected at different velocities and enabling the convection speed of the various scales to be determined using the phase $\Phi_k = \omega s_k/u_c^k(\omega)$. Again using the relationship between the space and time coordinates, this can be written as

$$\tau_{ij}^{k}(y,\omega') = \frac{1}{u_c^k(\omega)}\int_0^{+\infty} |\gamma_{ij}(\mathbf{y},\mathbf{s}_k,\omega')|\,\mathrm{d}\mathbf{s}_k. \tag{25}$$

This shows that a length scale evaluated using the modulus of the complex coherence function is not in fact a true length scale, but rather a product of the moving-frame time-scale and the convection velocity.

## 4. Modelling of the frequency-dependent scales

When the source term is expressed in the Proudman form $u_1^2(\mathbf{y},t)$ [12], the spectral functions are limited to the longitudinal component of the turbulent velocity field and the complexity of the problem is significantly reduced as a single correlation $r_{11}$ replaces the 36 quadrupole correlations $r_{ijkl}$. For the rest of the paper, the coherence length and time scales are restricted to the longitudinal component of the turbulence velocity field.

A number of models for the two point correlation function have been proposed in the literature. A form commonly used is the Gaussian model, because it is amenable to analytical and/or numerical manipulation. More complex models which account for the anisotropy or the inhomogeneity of the turbulence have been proposed in the literature [13–15], but while these have been shown to be more accurate, they often lead to extremely complicated analytical expressions. Of course these models can very easily be implemented numerically, and so are certainly attractive for those interested in effecting noise predictions from RANS data. For the sake of simplicity, a Gaussian model is used to demonstrate how frequency-dependent length and time scales can be related to their integral counterparts. The predictions are then compared with experimental data.

The two-point correlation function is thus taken as

$$r_{ij}(\mathbf{y},\mathbf{s}_k,\tau)=\exp\left[\frac{-\pi\tau^2}{\tau_{ij}^{k\,2}}\right]\exp\left[-\pi\frac{(s_k-U_c\tau)^2}{\Lambda_{ij}^{k\,2}}\right], \tag{26}$$

while the single-point correlation is modelled as

$$r_{ij}(\mathbf{y},\tau)=\exp\left[\frac{-\pi\tau^2}{\tau_{ij}^{y\,2}}\right], \tag{27}$$

where $\tau_{ij}^{y}$ denotes the fixed-frame integral time scale at location $\mathbf{y}$. The Fourier transform of these expressions gives the corresponding cross- and auto-power spectral density functions

$$S_{ij}(\mathbf{y},\mathbf{s}_k,\omega)=\frac{\tau_{ij}^{k}}{\sqrt{1+\alpha^2}}\exp\left[-\pi\frac{s_k^2}{\Lambda_{ij}^{k\,2}(1+\alpha^2)}\right]\exp\left[-\omega^2\frac{\tau_{ij}^{k\,2}}{4\pi(1+\alpha^2)}\right]\exp\left[-\mathrm{j}\omega\frac{\alpha\tau_{ij}^{k}s_k}{\Lambda_{ij}^{k}(1+\alpha^2)}\right],$$

$$S_i(\mathbf{y},\omega)=\tau_{ij}^{y}\exp\left[-\omega^2\frac{\tau_{ij}^{y\,2}}{4\pi}\right], \tag{28}$$

where $\alpha=U_c^k\tau_{ij}^k/\Lambda_{ij}^k$. When the Taylor hypothesis is applied this ratio is equal to unity, since the integral length and time scales are simply related by the convection speed. However, as noted by Wills [11], this assumption is generally not valid in the high speed jets.

In the particular case where the separation distance $s_k$ is zero, the single- and two-point correlation functions must be equal, and so by equating Eqs. (26) and (27) the moving and fixed axis time scales can be related by

$$\tau_{ij}^{k}=\tau_{ij}^{y}\sqrt{1+\alpha^2}. \tag{29}$$

For the spatial distances over which the turbulent field is appreciably correlated, the fixed-frame time scale can be considered as approximately constant. With this assumption (in effect the same $\tau_{ij}^{y}$ is used for the autospectra at the two locations) Eq. (28) can be used to write the complex coherence function defined in Section 3, as

$$\gamma_{ij}(\mathbf{y},\mathbf{s}_k,\omega)=\exp\left[-\pi\frac{s_k^2}{\Lambda_{ij}^{k\,2}(1+\alpha^2)}\right]\exp\left[-\mathrm{j}\omega\frac{\alpha}{1+\alpha^2}\frac{s_k}{\Lambda_{ij}^{k}}\right]. \tag{30}$$

Table 1
Jet exit conditions and values of the integral properties (respectively the longitudinal length and time scales, the convection velocity and the factor $\alpha = U_c\tau_{ij}/\Lambda_{ij}$) along the shear layer axis and end of the potential core

| Jet no. | $M_j$ | $T_j/T_o$ | $D$ (mm) | $\Lambda_{11}^1$ (mm) | $\tau_{11}^1$ (ms) | $U_c$ (m/s) | $\alpha$ |
|---|---|---|---|---|---|---|---|
| I | 0.75 | 1 | 50 | 27 | 0.69 | 146 | 2.25 |
| II | 0.75 | 2 | 50 | 18 | 0.46 | 182 | 2.30 |
| III | 0.9 | 1 | 50 | 19 | 0.62 | 137 | 2.20 |

By substituting this into Eqs. (20) and (25), that the frequency dependence of the space and time scales can be given by

$$\tau_{ij}^k(\mathbf{y},\omega) = \frac{1}{2}\tau_{ij}^k\sqrt{1+\frac{1}{\alpha^2}}, \tag{31}$$

$$\Lambda_{ij}^k(\mathbf{y},\omega) = \frac{\Lambda_{ij}\sqrt{1+\alpha^2}}{2}\exp\left[-\frac{\alpha^2{\tau_{ij}^k}^2\omega^2}{4(1+\alpha^2)}\right]. \tag{32}$$

These expressions can now be compared with two point experimental data.

## 5. Experimental set-up and analysis procedures

The high speed subsonic jet tests were conducted at the MARTEL facility of the CEAT (Centre d'Etudes Aerodynamiques et Thermiques) in Poitiers, France, using a 50 mm diameter nozzle with the jet mounted vertically and exhausting into free space. The jet conditions are given in Table 1 and more details of these experiments can be found in Ref. [15].

The measurements were obtained using a dual-beam LDV system with a traversing system designed and installed at the nozzle exit. A 5 W argon-ion laser, emitting both blue (488 nm) and green (514.5 nm) wavelengths was used in forward scatter to maximise signal to noise ratios and data rates. A pair of transmitting and receiving optic lenses were used, positioned faced to each other with their axis forming an angle of about 15° to provide the two-point measurements. Signals were processed by a TSI Doppler Signal Analyser. Both the potential core and shear layer were seeded simultaneously using silicon dioxide particles of 0.4 μm diameter in order to reduce velocity bias. The two-point/one-component measurements were made in non-coincident mode at both half-way and the end of the potential core region (about 2.5D and 5D downstream the nozzle exit) along the lip line of the nozzle. A schematic of the measurement positions is shown in Fig. 2. These measurements allow the correlation functions and spectra of the longitudinal velocity component to be determined and the length and time scales of the turbulence to be examined.

The temporal irregularity of LDV data means that the standard approaches used for calculation of auto and cross-correlation functions and for auto or cross-spectra cannot be applied. Although there are a number of different techniques by which correlation functions and spectra can be derived from LDV data, the two most common approaches are the slot correlation method and sample-and-hold reconstruction. Since the slot correlation method had been used for analysis of high speed jets [16] this technique was used here. The method is that proposed by van Maanen et al. [17], in which the fuzzy slotting technique of Nobach et al. [18] is combined with a local normalisation approach suggested by Tummers and Paschier [19]. Spectral estimation via slot correlation involves calculating all possible combinations of cross-product between the data points of two signals, which, plotted as a function of the associated time lags give an estimation of the cross-correlation function (CCF). The cross-products are then accumulated and averaged in equispaced bins (slots) in the correlation domain, giving a regularly discretised estimation of the cross-correlation function which can be subsequently windowed and Fourier transformed to give an estimate of the cross-power spectral density. The high variance associated with this approach can be mitigated by applying a triangular windowing function to each individual slot (fuzzy slotting), which allows cross-products from adjacent slots to contribute to the local

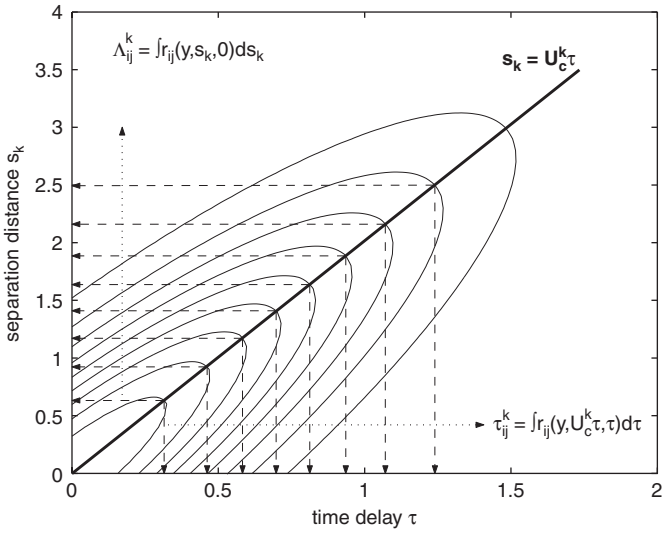


Fig. 2. Typical spatio-temporal correlation contours (arbitrary units) in the shear layer of a turbulent jet.

estimate, and to normalise each slot using only those data points which contribute to that estimate (local normalisation). The CCFs and the length and time scales for the measurements were derived from the auto and cross-spectra as detailed in Section 2.

## 6. Results

### 6.1. Frequency-dependent length scale

It has been shown in Section 3.1, that the frequency dependent length scale can be obtained from the real part of the complex coherence function defined by Eq. (19) (Fig. 2). A typical result, computed from the two-point LDV measurements is shown in Fig. 3 for an isothermal jet with a Mach number of 0.75. The measurement was made on the shear-layer axis and in the vicinity of the end of the potential core. The figure also shows the results from the analytical model given by Eq. (30). Agreement between the model and the experimental data is generally good with the exception of the very low frequencies. The spatial decay of the coherence functions is seen, not surprisingly to be strongly frequency dependent so that the smaller scales are coherent over smaller spatial extents than the larger scales. While not shown here, similar trends were found within the two other jet conditions tested.

Also noteworthy is the shape of the curves. In contrast with the correlation curves typical of two-point measurements, the bandlimited coherence curves display a greater dynamic with overshoots of between 0.5 and 1 both in the experimental data and the model depending on the frequency considered. This suggests that the bandlimited coherence function provides a means of extracting the dynamic of individual turbulent eddies of different sizes where this dynamic is similar to what one would expect from coherent vortical structures. It is important however to note that the curves in these figures are normalised and so they cannot be directly compared. In fact while the contribution of the 4 kHz component presents a very large dynamic its actual energy is far less than the principal energy carrying structures in the vicinity of 2 kHz. This result is consistent with the vortex model proposed by Lau et al. [20], in which the number of positive lobes corresponds to the number of times the eddies roll. The lower frequency components are thus seen to roll less than those associated with higher frequencies as would intuitively be expected. The larger structures do not have time to roll before becoming involved in a new event, such as pairing, leap-frogging or tearing. The smaller, higher frequency eddies on the other hand, being less sensitive to the large-scale dynamic of the jet may roll a number of times before dissipating. These observations are of some interest where the sound generation mechanism is

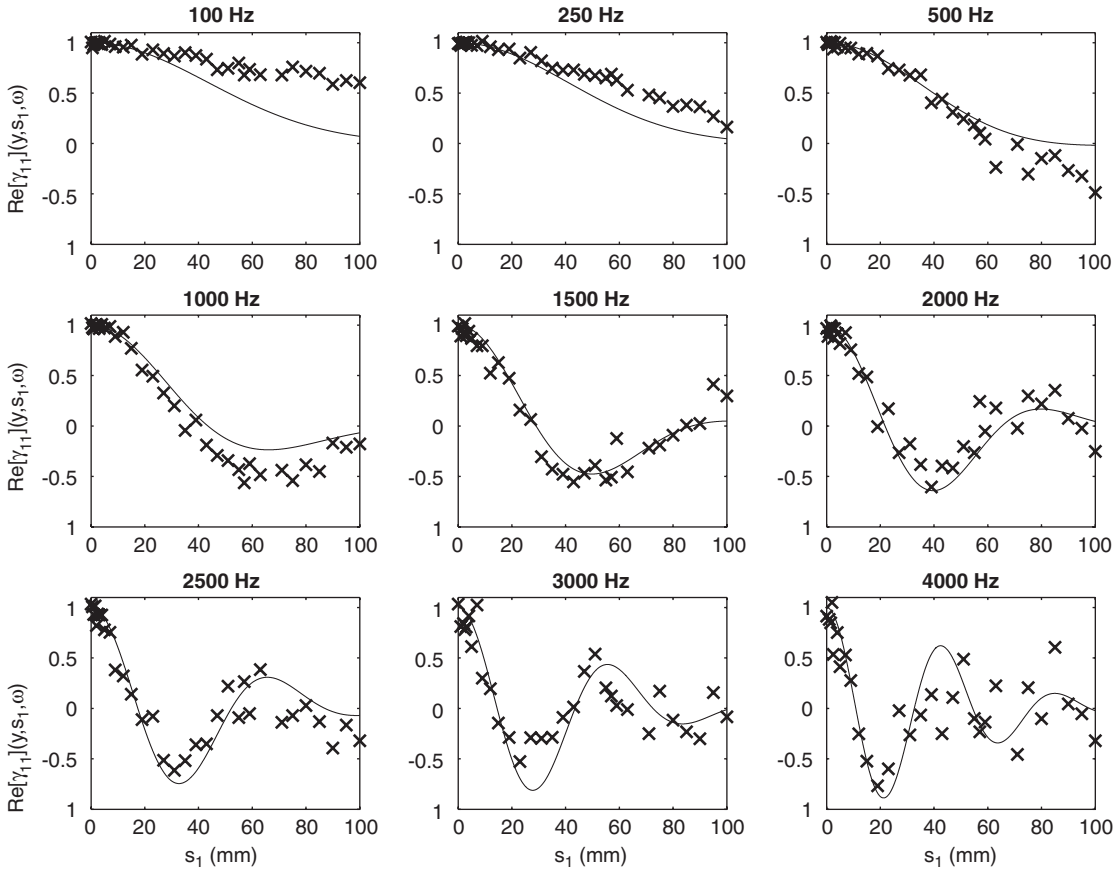


Fig. 3. Real part of complex coherence as a function of the separation distance $s_1$ at different frequencies in the Mach 0.75 isothermal jet. Location in the jet: half the potential core and shear layer axis. (×) Experimental results, (—) Eq. (30).

concerned as the source system can, as an alternative to the Lighthill form, be expressed in terms of vorticity of the flow [21]. The present results show a more explicit link between the vortical motions of various scales, the Lighthill stress tensor and the far-field sound. It can be seen thus how the spectral approach can provide improved insight to the structure of the turbulence, and of course via Lighthill's equation it will be possible to relate these characteristics of the flow structure to the radiated sound field.

The frequency dependence of the integral length scale is shown in Fig. 4 as a function of the Strouhal number, $St = fD/U_j$, for the three jets at different axial positions. The local power spectral density of the longitudinal turbulent velocity is also reported for each of these cases. A first observation is that the frequency dependence of the length scale is clear, showing a decrease with increasing Strouhal number according to a $-\frac{4}{5}$ law. Harper-Bourne [3] reported a similar trend for a frequency-dependent scale estimated using the magnitude of two-point CCF, which as discussed earlier is related to the moving-axis time scale, and Morris and Boluriaan [4] used a similar frequency dependence in a modelling approach with scale inversely proportional to the Strouhal number.

When plotted now as a Strouhal number $f\Lambda_{11}^1/U_j$, as reported in Fig. 5(a), the scale is found to increase towards a constant value at higher Strouhal numbers with a similar trend regardless of the jet exit velocity. In the case of the hot jet, the same tendency is observed but results show lower values. This tendency towards a constant value at higher Strouhal numbers indicates that a universal Strouhal number may exist for the smaller, higher frequency scales of the turbulence.[1] However this Strouhal number is not the same for heated

[1]We are indebted to one of our reviewers for pointing this out.

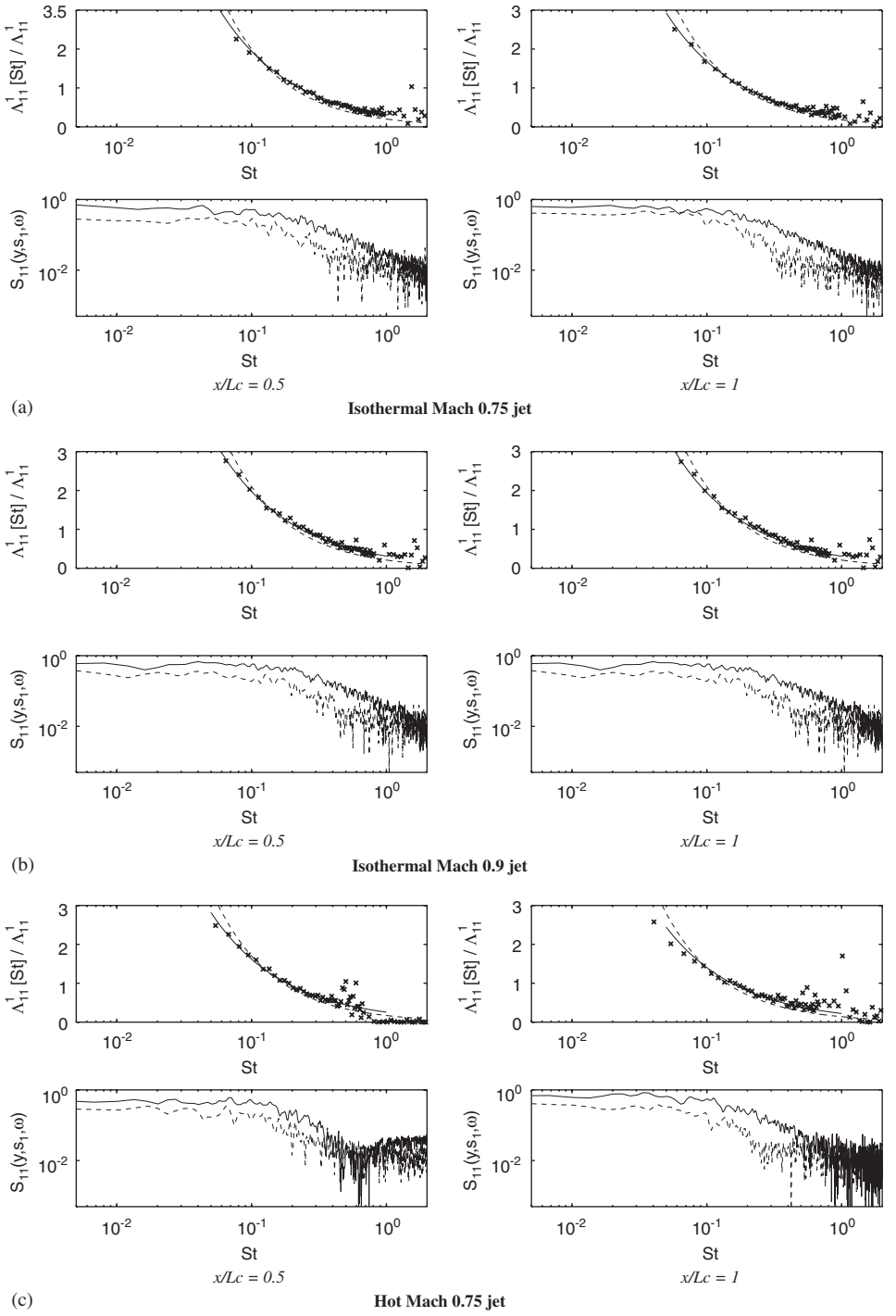


Fig. 4. Frequency dependent length scale (top sub-figures) and cross-power spectra (bottom sub-figures) as a function of the Strouhal number. Top figures: (×) experimental data, (—) $St^{-4/5}$ law and (- - -) $St^{-1}$ law. Bottom figures: (—) $s_1 = 0$ and (- - -) $s_1 = 1.8D$. Jet conditions: (a) isothermal Mach 0.75 jet; (b) isothermal Mach 0.9 jet; and (c) hot Mach 0.75 jet. Results obtained along the shear layer axis and (left column) half the potential core and (right column) end of the potential core.

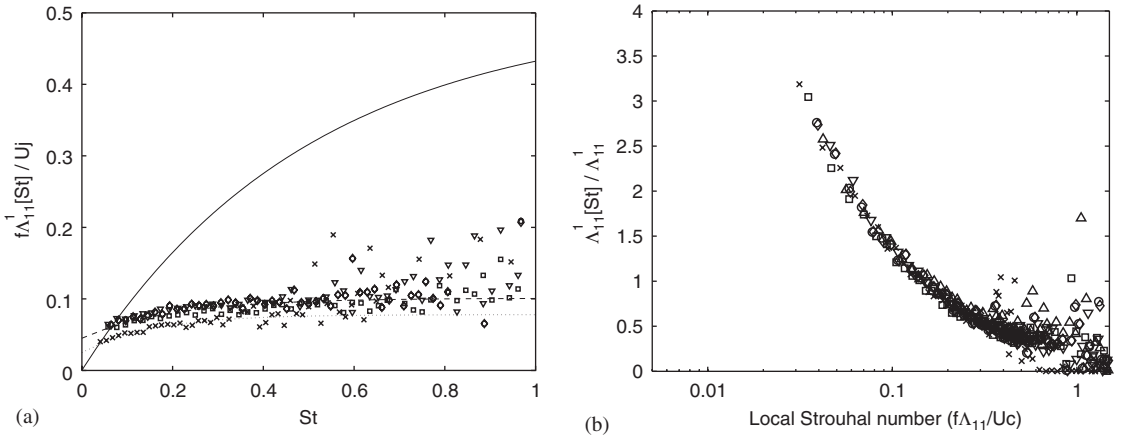


Fig. 5. Normalised frequency-dependent length scale as a function of: (a) the Universal Strouhal number; and (b) the Strouhal number defined as $fA^1_{11}/U_c$ for different jet exit conditions. Isothermal Mach 0.75 jet: (□) mid core, (▽) end core — isothermal Mach 0.9 jet: (○) mid core, (◇) end core — anisothermal Mach 0.75 jet: (△) mid core, (×) end core. Fitting curves: (—) Harper-Bourne [3], (- - -) $0.056(1-\exp(-4St))+0.045$ and (· · ·) $0.053(1-\exp(-6.5St))+0.025$.

and unheated flows. In the heated flow the Universal Strouhal number is slightly lower than in the unheated case. In order to collapse the heated and unheated cases the data must be plotted with the frequency dependent length scale normalised by the local integral length scale, and with the Strouhal number defined using the local convection velocity. This is shown in Fig. 5(b) where a good collapse of the data is observed.

The ability to collapse data from both hot and cold flows using the local integral length scale and the local convection velocity has important implications where jet noise modelling is concerned. It means that an estimate of the frequency dependence of the scales can be made using limited data available from RANS computations.

As mentioned earlier, the length scale used by Harper-Bourne [3] and Morris and Boluriaan [4] relates to a moving-axis time scale. When viewed in a moving reference frame a turbulence field decays much more slowly than when viewed in a fixed frame (i.e. the characteristic time scales are much larger), and this explains the large differences between the present results and those reported by Harper-Bourne, as shown in Fig. 5(a).

Finally, while the spectral resolution of the experimental data does not allow the frequency-dependent length scale to be obtained at low frequencies, a different behaviour in the low Strouhal number regime is observed when the model established in the previous section is applied. A typical comparison of the model prediction with the experimental results is shown in Fig. 6 where reasonably good agreement is found. When the frequency decreases, the model predicts a convergence of the length scale towards a constant value slightly higher than the integral length scale. However, it is important to note that this convergence of the frequency-dependent length scale is a consequence of the form initially chosen for the correlation function.

### 6.2. Frequency-dependent time scale

It was shown in Section 3.2 that the frequency-dependent time scale in the convected frame can be obtained using the modulus of the complex coherence function. A series of these curves extracted from the two-point measurements performed at the same location and in the same jet conditions as used for the length scales are shown in Fig. 7.

The same trends observed in the length scales are evident with the higher frequency eddies dissipating more rapidly than the lower frequencies. Although the magnitude of the complex coherence function is plotted with respect to a spatial coordinate, it is important to note that this quantity relates to the temporal dynamic of the turbulence components when viewed in the moving reference frame. Contrary to the trend found when the real part of the coherence is used for the length scales, no oscillation is observed for this. This is consistent with a

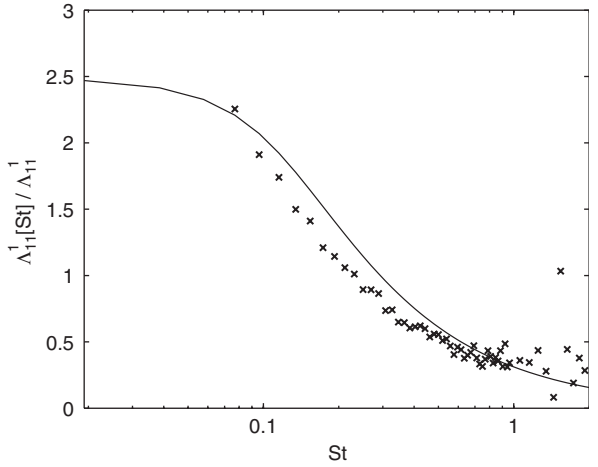


Fig. 6. Frequency-dependent length scale as a function of the Strouhal number in the isothermal Mach 0.75 jet: (×) experimental results and (—) integration over space of Eq. 30.

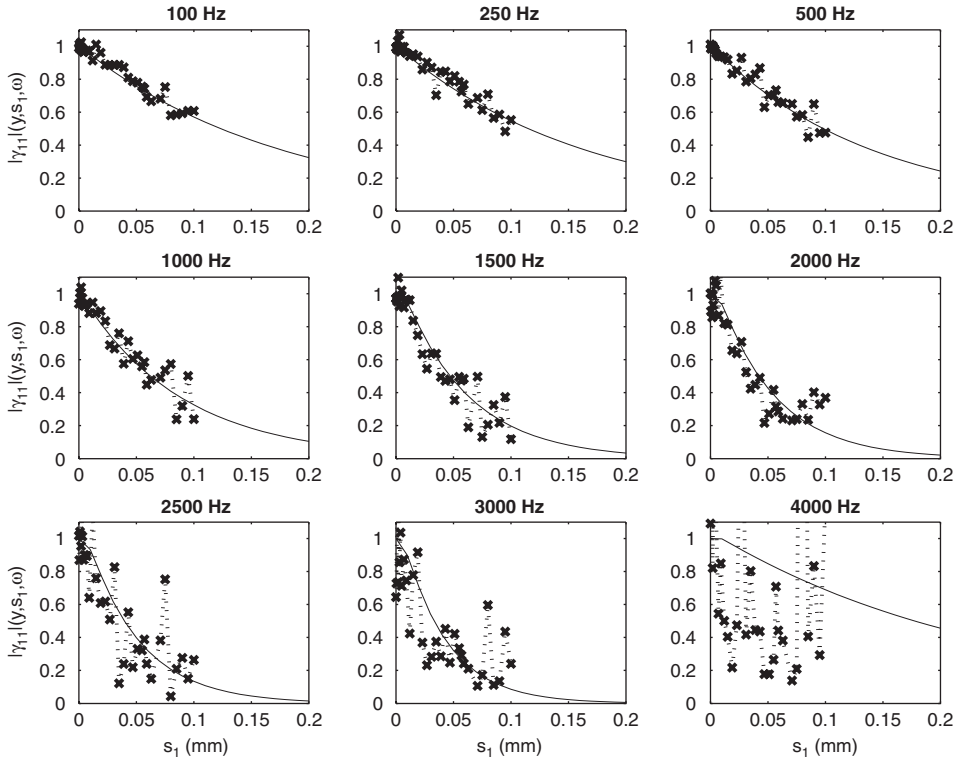


Fig. 7. Magnitude of complex coherence as a function of the separation distance for different frequencies. Results obtained in the Mach 0.75 isothermal jet along the shear layer axis and end of the potential core: (×) experimental results, (—) fitted data.

turbulence field viewed in a moving reference frame having a smaller dynamic than the field viewed in a fixed frame where a large part of the dynamic is related simply to convection of a quasi 'frozen' field past the fixed observation point.

Since the spatial resolution of the data is relatively poor and high variance can be observed, the data is fitted using an exponential function. As this model agrees well with the experimental data as can be seen in Fig. 7,

the frequency-dependent time scale is determined through integration of this function according to Eq. (25). The frequency dependence of the time scale is shown in Fig. 8 for the three jets tested. The general trend observed is similar to those seen for the length scales, higher frequency motion showing a shorter lifespan than lower frequency activity. Again, as discussed earlier, with more extensive measurements this kind of approach can be extremely useful when used in conjunction with an acoustic analogy, in order to determine the contributions to the far-field sound from the different spectral components of the turbulence.

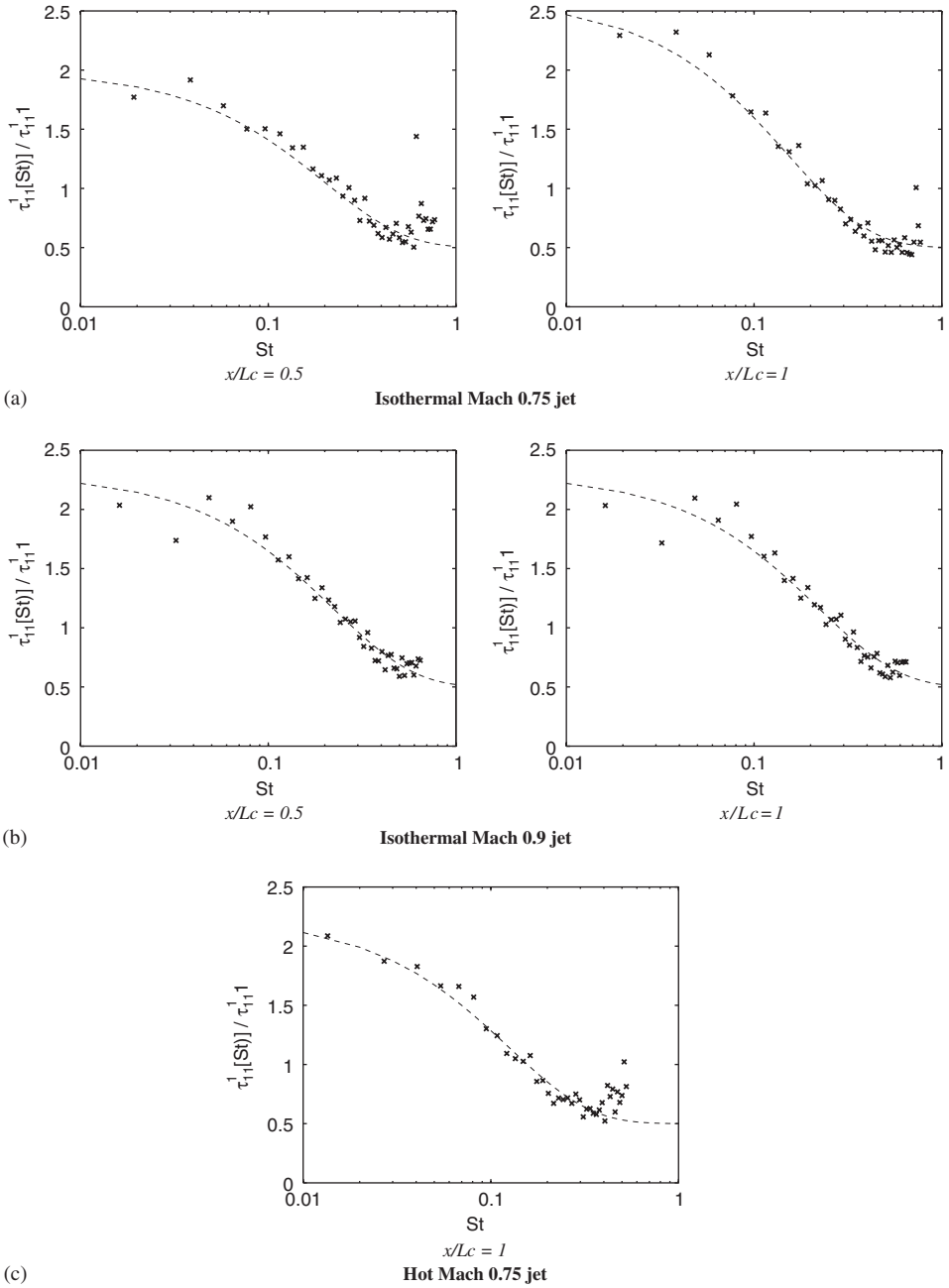


Fig. 8. Integral time scale as a function of the Strouhal number for different subsonic jet conditions: (a) isothermal Mach 0.75 jet; (b) isothermal Mach 0.9 jet; and (c) hot Mach 0.75 jet. Results obtained along the shear layer axis and (left column) half the potential core and (right column) end of the potential core. (×) Experimental data, (- - -) fitted line in a $\exp(-St/b) + c$ law where a,b and c are parameters.

Comparison of results obtained for the three different jet conditions, show how an increase of either the temperature or Mach number leads to a turbulence with smaller characteristic length and time scales.

### 6.3. Frequency-dependent convection velocity

The convection velocity is an extremely important quantity in the analysis and modelling of jet noise. Two effects are manifest. The first is a modification of the perceived sound frequency due to a Doppler shift. The second effect, so important in the jet-noise directivity pattern, is an amplification of the sound power radiated in the downstream direction. In effect cancellation between the respective poles of a quadrupole source mechanism is rendered less efficient by convection, and the effective integral scale of the quadrupole is increased in the axial direction leading to larger, more efficient sources for an observer in the downstream direction. It has been widely reported in the literature [9,16,22] how the convection velocity measured in a jet is found to vary both as a function of position and of frequency. This of course means that the efficiency of the turbulence in the generation of sound varies as a function of both spatial location and frequency. There are of course also important implications where our understanding of the turbulence dynamic alone is concerned, as identified by Wills [11] and Fisher and Davies [9]. Because the turbulence cannot be simply represented as a convected frozen pattern it is extremely difficult to relate the fixed-frame frequencies to the effective wavenumbers of the flow structure.

In the context of this study, where we are interested in the frequency dependence of the turbulence characteristics and the implications for the sound production mechanisms. The frequency dependence of the convection velocity means that different size eddies which are characterised by the frequency dependent length scale, with different characteristic frequencies (the frequency dependent moving-frame timescale) are convected at different velocities, and so in the context of Lighthill's acoustic analogy, this will lead to varying levels of efficiency and strength of the corresponding space–time source structure. As previously stated, a further study is necessary to more explicitly link these characteristics of the turbulence to the far-field sound.

The phase angle of the cross-spectrum is shown in Fig. 9 for a number of different separations, and it is from this that the convection velocity can be assessed as a function of frequency. The decrease with increasing separation in the spectral range over which the phase of the cross-spectrum is meaningful as it is indicative of the shorter lifespan of the small-scale, high frequency structures. The frequency dependence of the convection velocity is shown in Fig. 10 for the three different jet conditions. An increase of this quantity is found over the range of frequency examined. This suggests that the individual frequency turbulent components, while strongly related, have a random phase relative to the each other and convect downstream with a specific velocity.

While the convection velocities are globally slightly higher than those estimated by Fisher and Davies [9], the general trend of the data is in good agreement, and the absolute values agree extremely well with the

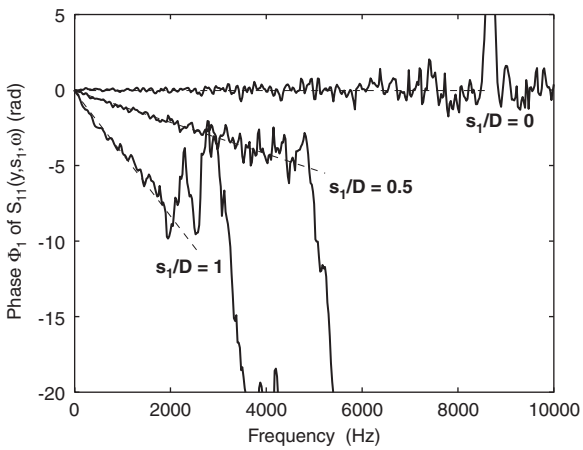


Fig. 9. Phase angle as a function of frequency for different separations (Mach 0.75 isothermal jet).

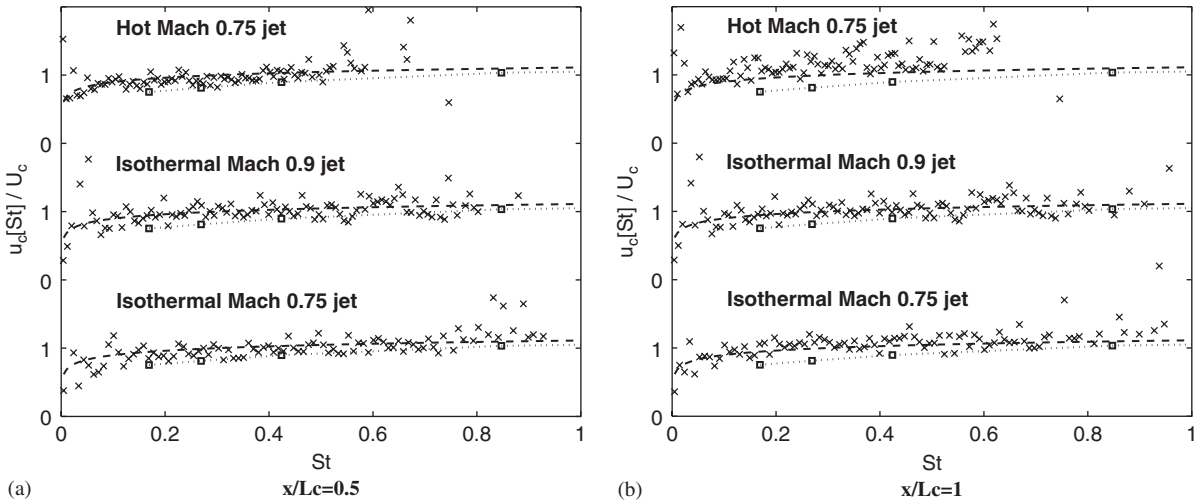


Fig. 10. Normalised convection speed as a function of the Strouhal number for different subsonic jet conditions and at two locations along the shear layer axis: (a) half of the potential core, (b) end of the potential core. (×) Experimental results, (· · □ · ·) Fisher and Davies [9], (- - -) Harper-Bourne [3].

measurements of Harper-Bourne [3] (Fig. 10). It should be mentioned that both authors used hot-wire anemometry, which for two-point turbulence measurements along axes parallel to the jet axis is problematic on account of the wake generated by the upstream wire. However, the good agreement of Harper-Bourne's measurements would seem to suggest that this has not in fact contaminated the measurement. The only other difference between our measurements and those of Fisher and Davies is the Reynolds number (present $Re \approx 1e06$, Fisher and Davies $Re \approx 2e05$), but again the Reynolds number of Harper-Bourne is similar to that of Fisher and Davies and yet the results agree well with those presented here.

The higher dispersion in the values at higher frequency corresponds to the $-\frac{5}{3}$ region of the velocity spectra where on account of the lower spectral power of the velocity signal, the signal-to-noise ratio of the measurement deteriorates. Nevertheless, the general trend would suggest that the high frequency components are convected with a velocity slightly higher than the local convection velocity. Furthermore, the results suggest that the classical convection velocity amounts to an average of the speeds at which the different constituents of the turbulent field are convected downstream, showing that this quantity is governed more by the mean flow than by the intrinsic properties of the turbulence.

## 7. Conclusion

The frequency dependence of the turbulence length and time scales for a subsonic jet has been established analytically. It has been shown how the real part of the complex coherence function obtained from two-point measurements of the turbulence velocity gives the frequency dependence of the space scale, whilst the modulus gives the time scale dependence and the convection speed is obtained from the phase. A model which relates this frequency dependence to the integral scales of the turbulence via a simple Gaussian form for the longitudinal correlation coefficient has also been developed. The frequency dependent scales have been evaluated from two-point measurements in hot and isothermal high-speed subsonic jets using LDV and good agreement has been found between the experimental data and the analytical model.

Both the length and time scales decrease as the Strouhal number increases. In particular, the frequency dependent length scale for all three jets reported was found to be proportional to the Strouhal number to the power of $-\frac{4}{5}$ suggesting that the turbulence has a universal Strouhal number dependence. The convection speeds were found to increase with frequency so that the smaller scales move more rapidly than the larger ones.

The results of this paper indicate how modelling procedures for noise predictions can include frequency dependence to provide for a more sophisticated use of the acoustic analogy for the prediction of jet noise.

## Acknowledgements

The experiments described were performed as part of the project JEAN (Jet Exhaust Aerodynamics and Noise) funded under the EU FP6 programme as contract no. G4RD-CT2000-00313.

## References

[1] M.J. Lighthill, On sound generated aerodynamically: I. General theory, *Procedure of the Royal Society* A (211) (1952) 558–564.
[2] A.A. Townsend, *The Structure of Turbulent Shear Flow*, second ed., Cambridge University Press, Cambridge, 1976.
[3] M. Harper-Bourne, Jet noise turbulence measurements, *AIAA/CEAS 9th Aeroacoustics Conference*, 2003, AIAA Paper 2003–3214.
[4] P.J. Morris, S. Boluriaan, The prediction of jet noise from CFD data, *AIAA/CEAS 10th Aeroacoustics Conference*, 2004, AIAA Paper 2004–2977.
[5] R.H. Self, Jet noise prediction using the Lighthill acoustic analogy, *Journal of Sound and Vibration* 275 (2004) 757–768.
[6] C. Durant, G. Robert, P.J.T. Filipi, P.O. Mattei, Vibroacoustic response of a thin cylindrical shell excited by a turbulent internal flow: comparison between numerical prediction and experimentation, *Journal of Sound and Vibration* 229 (2000) 1115–1155.
[7] M.J. Lighthill, An estimate of the covariance of $T_{xx}$ without using statistical assumptions, In: J.C. Hardin, M.Y. Hussaini (Eds.), *Computational Aeroacoustics*, ICASE/LaRC Series, 1993, pp. 112–113.
[8] J.B. Freund, Noise source turbulence statistics and the noise from a Mach 0.9 jet, *Physics of Fluids* 15 (6) (2003) 1788–1799.
[9] M.J. Fisher, P.O.A.L. Davies, Correlation measurement in a non-frozen pattern of turbulence, *Journal of Fluids Mechanics* 18 (1964) 97–116.
[10] J.L. Lumley, K. Takeuchi, Application of central-limit theorems to turbulence and higher-order spectra, *Journal of Fluids Mechanics* 74 (3) (1976) 433–468.
[11] J.A.B. Wills, On convection velocities in turbulent shear flows, *Journal of Fluid Mechanics* 20 (3) (1964) 417–432.
[12] I. Proudman, The generation of noise by isotropic turbulence, *Procedure of the Royal Society A* (214) (1952) 119–132.
[13] W.J. Devenport, C. Muthanna, R.M.S. Clegg, Two-point descriptions of wake turbulence with application to noise prediction, *AIAA Journal* 39 (12) (2001) 2302–2307.
[14] D. O'Hara, N. Andersson, P. Jordan, M. Billson, L. Edison, L. Davidson, A hybrid analysis methodology for improved accuracy in low cost jet noise modelling, *33rd International Congress and Exposition on Noise Control Engineering*, *Inter-Noise Conference*, Prague, Czech Republic, 2004.
[15] P. Jordan, Y. Gervais, Modelling self and shear noise mechanisms in inhomogeneous, anisotropic turbulence, *Journal of Sound and Vibration* 279 (2005) 529–555.
[16] F. Kerhervé, P. Jordan, Y. Gervais, J.-C. Valière, P. Braud, Two-point laser Doppler velocimetry measurements in a Mach 1.2 cold supersonic jet for statistical aeroacoustic source model, *Experiments in Fluids* 37 (2004) 419–437.
[17] H.R.E. van Maanen, H. Nobach, L.H. Benedict, Improved estimator for the slotted autocorrelation function of randomly sampled LDA data, *Measurement in Science and Technology* 10 (1999) L4–L7.
[18] H. Nobach, Local time estimation for the slotted correlation function of randomly LDA data, *Experiments in Fluids* 32 (2002) 337–345.
[19] M.J. Tummers, D.M. Passchier, Spectral estimation using a variable window and slotting technique with local normalization, *Measurements in Science and Technology* 7 (1996) 1541–1546.
[20] J.C. Lau, P.J. Morris, M.J. Fisher, Measurements in subsonic and supersonic jets, *Journal of Sound and Vibration* 22 (4) (1979) 379–406.
[21] M.S. Howe, Contributions to the theory of aerodynamic sound, with applications to excess jet noise and the theory of the flute, *Journal of Fluid Mechanics* 71 (14) (1975) 625–773.
[22] P.O.A.L. Davies, M. Fischer, M. Barrat, The characteristics of turbulence in the mixing region of a round jet, *Journal of Fluid Mechanics* 15 (1963) 337–367.